

Springer Geology

Vladimir Karev · Dmitry Klimov  
Konstantin Pokazeev *Editors*

# Physical and Mathematical Modeling of Earth and Environment Processes

3rd International Scientific School for  
Young Scientists, Ishlinskii Institute  
for Problems in Mechanics of Russian  
Academy of Science

 Springer

**Springer Geology**

The book series Springer Geology comprises a broad portfolio of scientific books, aiming at researchers, students, and everyone interested in geology. The series includes peer-reviewed monographs, edited volumes, textbooks, and conference proceedings. It covers the entire research area of geology including, but not limited to, economic geology, mineral resources, historical geology, quantitative geology, structural geology, geomorphology, paleontology, and sedimentology.

More information about this series at <http://www.springer.com/series/10172>

Vladimir Karev · Dmitry Klimov  
Konstantin Pokazeev  
Editors

# Physical and Mathematical Modeling of Earth and Environment Processes

3rd International Scientific School for Young  
Scientists, Ishlinskii Institute for Problems  
in Mechanics of Russian Academy of Science

*Editors*

Vladimir Karev  
Institute for Problems in Mechanics  
of the Russian Academy of Sciences  
(IPMech RAS)  
Moscow  
Russia

Konstantin Pokazeev  
Faculty of Physics  
Lomonosov Moscow State University  
Moscow  
Russia

Dmitry Klimov  
Institute for Problems in Mechanics  
of the Russian Academy of Sciences  
(IPMech RAS)  
Moscow  
Russia

ISSN 2197-9545

Springer Geology

ISBN 978-3-319-77787-0

<https://doi.org/10.1007/978-3-319-77788-7>

ISSN 2197-9553 (electronic)

ISBN 978-3-319-77788-7 (eBook)

Library of Congress Control Number: 2018937380

© Springer International Publishing AG, part of Springer Nature 2018

This work is subject to copyright. All rights are reserved by the Publisher, whether the whole or part of the material is concerned, specifically the rights of translation, reprinting, reuse of illustrations, recitation, broadcasting, reproduction on microfilms or in any other physical way, and transmission or information storage and retrieval, electronic adaptation, computer software, or by similar or dissimilar methodology now known or hereafter developed.

The use of general descriptive names, registered names, trademarks, service marks, etc. in this publication does not imply, even in the absence of a specific statement, that such names are exempt from the relevant protective laws and regulations and therefore free for general use.

The publisher, the authors and the editors are safe to assume that the advice and information in this book are believed to be true and accurate at the date of publication. Neither the publisher nor the authors or the editors give a warranty, express or implied, with respect to the material contained herein or for any errors or omissions that may have been made. The publisher remains neutral with regard to jurisdictional claims in published maps and institutional affiliations.

Printed on acid-free paper

This Springer imprint is published by the registered company Springer International Publishing AG part of Springer Nature

The registered company address is: Gewerbestrasse 11, 6330 Cham, Switzerland

# Preface

This book, entitled “Physical and Mathematical Modeling of Earth and Environment Processes. 3rd International Scientific School for Young Scientists, Ishlinskii Institute for Problems in Mechanics of Russian Academy of Sciences” is the result of a collaborative work in the frame of the youth scientific conference held at the Ishlinskii Institute for Problems in Mechanics of RAS on November 1–3, 2017. This forum is held on a regular basis and causes great interest in the scientific community. For the third year in a row, more than one hundred scientists have taken part in it, two-thirds of who are young researchers.

The 3rd School, as well as the previous two, promoted to the solution of fundamental scientific problems arising in the study of natural processes in different media, the impact of anthropogenic activities on the environment. Intensive development of research in these areas is due to several factors. The widespread introduction of computer technology has allowed beginning calculation of complex phenomena, previously unavailable for analysis. Creation and improvement of a new generation of geophysical instruments and remote observing systems based on the ship, aircraft, and satellite allowed to obtain a large amount of data to objectively reflect the picture of the processes. International activities including the youth scientific schools are certainly an effective tool for exchange of information and the organizing of interdisciplinary research of environment processes.

One of the central topics for the School is associated with the elaboration of scientific bases of oil and gas production technologies. The creation of new breakthrough approaches to the development of hydrocarbon fields is very important today and requires the involvement of young minds and strength.

During all three Schools, participant’s reports were traditionally accompanied by active discussions which lasted beyond the end of the program sessions. The most interesting and promising areas of research were recognized in the following: the development of geomechanical approach to solving the problems of oil and gas production, physical and mathematical modeling of deformation and fracture of solid media and study of their interaction on the seepage, creation effective mathematical models and experimental base for research of flows in complex heterogeneous liquids, environmental issues, the study of the anthropogenic contribution

to the dynamics of natural systems. As a result of the work of the third School, it was decided to publish the most interesting reports as the book.

The book presents the results of theoretical and experimental research of processes in the atmosphere, oceans, the lithosphere and their interaction; environmental issues; problems of human impact on the environment; methods of geophysical research. The conference papers included in the book describe the studies on the dynamics of natural systems, the human contribution to naturally occurring processes, laboratory modeling of these processes, and testing of new developed physical and mathematical models.

A wide range of problems associated with the production of hydrocarbons is the central topic of the book. A special attention is paid to the geomechanical approach to solving these problems. An alternative to the use of hydrocarbons as a main source of energy on the planet in the coming decades is unlikely to be found. At the same time, the resource base of hydrocarbons is quickly depleted, and new non-traditional sources are required. Among them, there is shale oil and gas, Arctic hydrocarbon reserves gas hydrates, as well as oil and gas from deep horizons (more than 5.5 km). “Deep oil” may become the most promising source of expanding the resource base of hydrocarbons according to many experts. At the same time, environmental problems are becoming increasingly acute, and the need arises to create environmentally friendly technologies. The basis for the creation of such technologies can become a geomechanical approach based on the use of a huge reserve of elastic energy stored in a rock mass by controlling the stress–strain state of the formation. The book includes the new results of the experimental and theoretical modeling deformation, destruction and filtration processes in the rocks related to issues of creating scientific fundamentals for new hydrocarbon production technologies. The investigation of the dependence of well stability and permeability of rocks on the stress–strain state in conditions of high rock pressure is represented too.

Our book

- Enriches the understanding of the geophysical processes taking place in various environments (lithosphere, hydrosphere, atmosphere), including anthropogenic, and promotes to the intensification of their studying.
- Includes the results of theoretical and experimental studies on the development of the geomechanical approach to creating new technologies in the field of hydrocarbon production based on controlling the stress–strain state in the reservoir.
- Contains the results of recent research in the field of interactions of the lithosphere, atmosphere, and hydrosphere of various scales, energy exchange of the atmosphere and the ocean, including under anthropogenic influences.
- Expands the understanding problems of providing oil and gas wells stability in the process of their construction and operation, increasing the efficiency of hydrocarbon production including on the ocean shelf, thereby raising the efficiency of training specialists in oil reservoir physics.

- Presents modern methods of research and modeling of various processes in environment, means and ways of monitoring of natural systems, methods of research and forecasting of natural and man-made disasters, and ways to eliminate their consequences.
- Proposes new physical and mathematical models of processes occurring in the environment, both natural and anthropogenic, as well as elaboration of existing ones.
- Contains additional material for specialists working in the oil and gas industry to expand, improve, and disseminate new acknowledgments in this field.

Program Committee of the School, which included the leading scientists on the scientific directions of the School, has conducted peer review of the papers submitted to the book and produced a competitive selection. Ninety-eight works were submitted. As a result of double-blind peer review, 38 papers were selected.



# Organization

## Organizers of the School

Ishlinskii Institute for Problems in Mechanics of Russian Academy of Sciences  
Faculty of Physics of Lomonosov Moscow State University

## Organizing Committee

V. I. Karev (Chairman)	Ishlinskii Institute for Problems in Mechanics of RAS, Russia
K. V. Pokazeev (Dep. Chair)	Lomonosov Moscow State University, Russia
A. Yu. Volkova	Lomonosov Moscow State University, Russia
Yu. F. Kovalenko	Ishlinskii Institute for Problems in Mechanics of RAS, Russia
A. L. Levitin	Ishlinskii Institute for Problems in Mechanics of RAS, Russia
E. V. Stepanova	Ishlinskii Institute for Problems in Mechanics of RAS, Russia
K. B. Ustinov	Ishlinskii Institute for Problems in Mechanics of RAS, Russia
T. O. Chaplina (Sc. Secretary)	Lomonosov Moscow State University, Russia
N. I. Shevtsov	Ishlinskii Institute for Problems in Mechanics of RAS, Russia

## Program Committee

A. A. Babanin	Swinburne University of Technology, Australia
T. O. Chaplina (Sc. Secretary)	Lomonosov Moscow State University, Russia
V. V. Fadeev	Lomonosov Moscow State University, Russia
N. N. Filatov	Northern Water Problems Institute Karelian Research Centre, Russia

A. N. Dmitrievsky	Institute of Oil and Gas Problems of RAS, Russia
R. V. Goldstein <sup>1</sup>	Ishlinskii Institute for Problems in Mechanics of RAS, Russia
V. I. Karev (Dep. Chair)	Ishlinskii Institute for Problems in Mechanics of RAS, Russia
D. M. Klimov (Chairman)	Ishlinskii Institute for Problems in Mechanics of RAS, Russia
Yu. F. Kovalenko	Ishlinskii Institute for Problems in Mechanics of RAS, Russia
V. E. Kunitsyn	Lomonosov Moscow State University, Russia
V. B. Lapshin	Institute of Applied Geophysics, Russia
Yu. G. Leonov	Geological Institute of RAS, Russia
V. P. Matveenko	Institute of Continuous Media Mechanics of the Ural Branch of RAS, Russia
R. I. Nigmatulin	Shirshov Institute of Oceanology of RAS, Russia
V. N. Nosov	Vernadsky Institute of Geochemistry and Analytical Chemistry of RAS, Russia
K. V. Pokazeev (Dep. Chair)	Lomonosov Moscow State University, Russia
A. A. Soloviev	Lomonosov Moscow State University, Russia
B. G. Tarasov	University of Western Australia
P. O. Zavyalov	Shirshov Institute of Oceanology of RAS, Russia
A. S. Zapevalov	Marine Hydro-Physical Institute of RAS, Russia
V. N. Zyryanov	Water Problems Institute of RAS, Russia

## Sponsors

Russia Foundation for Basic Research (project № 17-31-10210)

Russian Academy of Science Presidium Program for Fundamental Research I.4P «Deposits of strategic resources in Russia: innovative approaches for their prediction, evaluation and production. Oil from the deep horizons of sedimentary basins as the source of replenishment of resource base of hydrocarbons: theoretical and applied aspects»

## School Venue

Ishlinskii Institute for Problems in Mechanics of RAS  
119526, Russia, Moscow, Vernadskogo Avenue, 101-1

---

<sup>1</sup>R. V. Goldstein died on 24/09/2017.

# Contents

<b>The Tyrrhenian Continent Ragmentation</b> . . . . .	1
Al. A. Schreider, A. A. Schreider, and A. E. Sazhneva	
<b>Long Waves Influence on Polarization Ratio for Microwave Backscattering from the Sea Surface</b> . . . . .	9
Alexandr Zapevalov	
<b>Elimination of Hydrocarbons Spills on Water Objects and Fluorescent Diagnostics of Water Purenness</b> . . . . .	17
T. O. Chaplina and E. V. Stepanova	
<b>Investigations of Internal Waves in the Seas of Russia and in the Central Atlantic</b> . . . . .	28
K. S. Grigorenko and S. M. Khartiev	
<b>Critically Stressed Fractures and Their Relation to Elastic Moduli</b> . . . . .	35
Nikita Vladislavovich Dubinya and Ilya Vladimirovich Fokin	
<b>Mechanical Properties of Thin Films of Coals by Nanoindentation</b> . . . . .	45
Elena Kossovich, Svetlana Epshtein, Nadezhda Dobryakova, Maxim Minin, and Darya Gavrilova	
<b>Using the Variational Approach and Adjoint Equations Method Under the Identification of the Input Parameter of the Passive Admixture Transport Model</b> . . . . .	51
Sergey Germanovich Demyshev, Vladimir Sergeevich Kochergin, and Sergey Vladimirovich Kochergin	
<b>Mechanisms Accounting for Interannual Variability of Advective Heat Transport in the North Atlantic Upper Layer</b> . . . . .	62
A. B. Polonsky and P. A. Sukhonos	
<b>Convective Jets: Volcanic Activity and Turbulent Mixing in the Boundary Layers of the Atmosphere and Ocean</b> . . . . .	71
Alexander Vulfson, Oleg Borodin, and Petr Nikolaev	

<b>Theoretical and Experimental Evaluation of Formation Fluid Composition Influence on Filtration and Elastic Properties of Porous Media</b> . . . . .	84
Daniil Karmanskiy and Andrey Maltsev	
<b>Synchronous Changes of Geophysical Fields in the Earth's Near-Surface Zone</b> . . . . .	90
Svetlana Riabova and Alexander Spivak	
<b>Vertical Mass Transport by Weakly Nonlinear Inertia-Gravity Internal Waves</b> . . . . .	99
A. A. Slepyshev and D. I. Vorotnikov	
<b>Field Investigation and Numerical Simulation of Wind-Wave Interaction at the Middle-Sized Inland Reservoirs</b> . . . . .	112
G. A. Baydakov, A. M. Kuznetsova, V. V. Papko, A. A. Kandaurov, M. I. Vdovin, D. A. Sergeev, and Yu. I. Troitskaya	
<b>Multidecadal Variability of Hydro-Thermodynamic Characteristics and Heat Fluxes in North Atlantic</b> . . . . .	125
N. A. Diansky and P. A. Sukhonos	
<b>Reconstruction of Hydrophysical Fields in the Coastal Region of the Black Sea on the Basis of Hydrodynamic Model with Assimilation of Observational Data</b> . . . . .	138
Demyshev Sergei and Evstigneeva Natalia	
<b>The Vertical Turbulent Exchange Features in the Black Sea Active Layer</b> . . . . .	148
A. S. Samodurov and A. M. Chukharev	
<b>Model of Oscillations of Earth's Poles Based on Gravitational Tides</b> . . .	157
S. A. Kumakshev	
<b>Laboratory Modeling of Ring Geophysical Structures</b> . . . . .	164
B. Shvilkin	
<b>Principles of Controlling the Apparatus Function for Achieving Super-Resolution in Imagers</b> . . . . .	171
E. N. Terentiev, N. E. Terentiev, and I. I. Farshakova	
<b>A Regular System of Vortices in a Circular Stratified Flow Behind the Edge of a Rotating Disk</b> . . . . .	183
Roman N. Bardakov	
<b>Comparison of Empirical Sea-Surface Slopes Probability Densities for the Purposes of Satellite Sounding</b> . . . . .	191
Nick Evgenievich Lebedev and Alexandr Sergeevich Zapevalov	

**Mathematical Modeling of Thermomechanical Behavior of Porous Impermeable Medium with Active Filler** . . . . . 201  
 M. V. Alekseev, E. B. Savenkov, and N. G. Sudobin

**Evaluation of the Temporal Dynamics of Oceanic Eddies with Initial Peripheral Rate Shift** . . . . . 207  
 Alexander Alexeyevich Solovyev and Dmitry Alexandrovich Solovyev

**Reservoir Proxy Model as a Part of Geo-Technological Model of Gas Fields and Underground Gas Storages** . . . . . 217  
 Sergey A. Kirsanov, Andrey V. Chugunov, Oleg S. Gatsolaev, Yan S. Chudin, Ivan A. Fedorov, Aleksey A. Kontarev, and Alexandra P. Popovich

**Understanding of Rock Material Behavior Under Dynamic Loadings Based on Incubation Time Criteria Approach** . . . . . 233  
 A. N. Martemyanov and Yu. V. Petrov

**Analytical Research of Character of Relative Permeability Function Under Unsteady Two-Phase Filtration** . . . . . 249  
 D. U. Semiglasov and V. M. Maximov

**Estimation of the Hydraulic Fracture Propagation Rate in the Laboratory Experiment** . . . . . 259  
 M. Trimonova, E. Zenchenko, N. Baryshnikov, S. Turuntaev, P. Zenchenko, and A. Aigozhieva

**Paleomagnetism of Some Basalts Samples from the Red Sea Rift Zone** . . . . . 269  
 V. I. Maksimochkin and L. R. Preobrazhenskii

**Influence of Hydrodynamic Perturbations on Dispersion Characteristics of a Near-Water Aerosol** . . . . . 282  
 V. N. Nosov, S. G. Ivanov, V. I. Pogonin, V. I. Timonin, N. A. Zavyalov, E. A. Zevakin, and A. S. Savin

**A Comparative Analysis of Optical Methods for Detection and Prediction of Radionuclides Migration in the Geosphere** . . . . . 289  
 B. P. Yakimov, G. S. Budylin, V. G. Petrov, V. V. Fadeev, S. N. Kalmykov, S. A. Evlashin, and E. A. Shirshin




**Advanced Procedure for Estimation of Phytoplankton Fluorescence Quantum Yield Using Remote Sensing Data: A Comparative Study of the Amundsen Sea Polynyas** . . . . . 298  
 Elena E. Nikonova, Evgeny A. Shirshin, Victor V. Fadeev, and Maxim Y. Gorbunov

**The Exact Mathematical Models of Nonlinear Surface Waves** . . . . . 305  
 Anatoly Kistovich

<b>Numerical Analysis and Prediction of the Consequences of Natural and Technological Impacts in Coastal Areas of the Azov Sea . . . . .</b>	<b>317</b>
T. Ya. Shul'ga, S. M. Khartiev, and A. R. Ioshpa	
<b>The Problem of Forecasting of Vertical Temperature Distribution in Inland Hydrophysical Objects with Experimental Data . . . . .</b>	<b>327</b>
D. Gladskikh, D. Sergeev, G. Baydakov, I. Soustova, and Yu. Troitskaya	
<b>Modeling Geomechanical Processes in Oil and Gas Reservoirs at the True Triaxial Loading Apparatus . . . . .</b>	<b>336</b>
V. I. Karev, D. M. Klimov, and Yu. F. Kovalenko	
<b>Modeling of Deformation and Filtration Processes Near Wells with Emphasis of their Coupling and Effects Caused by Anisotropy . . .</b>	<b>350</b>
V. I. Karev, D. M. Klimov, Yu. F. Kovalenko, and K. B. Ustinov	
<b>Effect of a Tidal Wave Caused by Large Gliding Satellite on Formation of 220 km Seismic Boundary and Split of the Mantle into Blocks . . . . .</b>	<b>360</b>
S. Kasyanov and V. Samsonov	
<b>Influence of Baroclinicity on Sea Level Oscillations in the Baltic Sea . . .</b>	<b>371</b>
Evgeny Zakharchuk, Natalia Tikhonova, Anatoly Gusev, and Nikolay Diansky	
<b>Author Index . . . . .</b>	<b>381</b>



# The Tyrrhenian Continent Ragmentation

Al. A. Schreider<sup>1</sup> , A. A. Schreider<sup>2</sup>  , and A. E. Sazhneva<sup>2</sup> 

<sup>1</sup> Research Institute of Economics and Management in Gas Industry,  
NIIgazekonomika Company Ltd., Moscow, Russia

<sup>2</sup> Institute of Oceanology, Russian Academy of Sciences, Moscow, Russia  
aschr@ocean.ru

**Abstract.** In the geological past, there was a continental formation in the place of the Tyrrhenian-Ligurian basin, that included Sicily, Sardinia, Corsica, and the Apennines in the southwest of the Italian peninsula. The stretching processes led to rifting, passing into diffuse spreading with the fragmentation of this formation. Calculation of Eulerian poles and rotation angles in the context of complex geological and geophysical interpretation of bottom geomorphology allowed to restore the spatial position of the axes of the initial split of the continental formation and to describe the kinematics of the microplates of analyzed region.

**Keywords:** West mediterranean paleogeodynamics · Tyrrhenian continent  
Euler poles

## 1 Introduction

The tectonic development of the western Mediterranean is inseparably linked with the multi-scale migration and rotations of the different age microplates of the continental and oceanic lithosphere [4, 5, 9, 13, 14, 16, 17]. Among the most important tectonic elements of this region include the Tyrrhenian Sea surrounding are such continental blocks as Corsica, Sardinia, Sicily and Apennine peninsula (Fig. 1). It is important to note that the geological and geophysical data accumulated to date do not contradict with the most diverse, sometimes mutually exclusive, paleogeodynamic constructions.

## 2 Tectonic Setting Peculiarities

In work [12] it is asserted that in the interval 170-67 million years ago the continental block uniting the islands of Corsica and Sardinia (hereinafter referred as the block CS) adjoined the Iberian Peninsula to the south of the Pyrenees. At a considerable distance from CS Sicily was located, and still further to the east of Sicily there were fragments of the structure of the modern Apennine peninsula. In contrast to that study, in [15] the block of CS 140 million years ago adjoined the Iberian Peninsula to the north of the Pyrenees. Sicily was located east of Corsica and further south of it was situated the south-western fragment of the modern Apennine peninsula. According to the data of [9], the rotation of the CS to its present day meridional position occurs successively for the last 30 million years, and it was shown in [10] that this rotation takes place only in

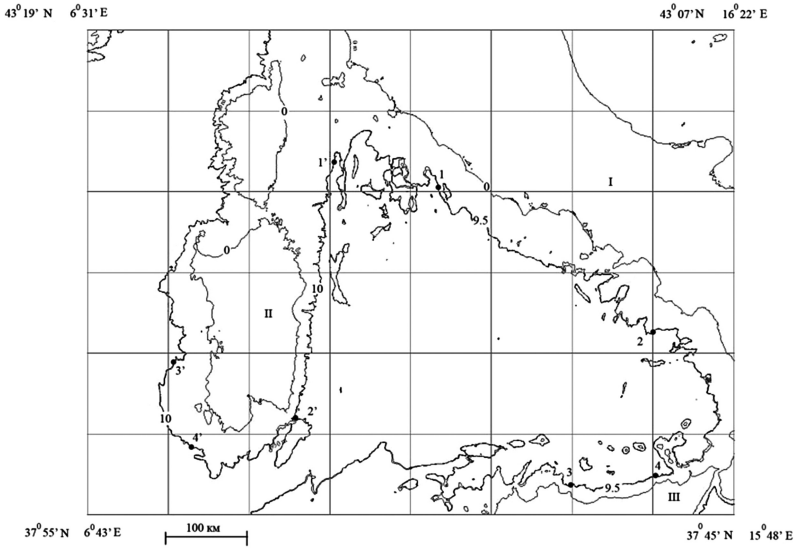


**Fig. 1.** The present day geographical position of the Apenninian peninsula (I), Corsica and Sardinia - block CS (II) and Sicily (III) along the periphery of the Tyrrhenian Sea. The position of the ends (points 1 and 2, 3 and 4) of the 0.95 km segments isobaths are shown, as well as the position of the conjugate sections of the 1 km isobaths ends (points 11 and 21, 31 and 41). Depths are in hundreds of meters according to [20].

the last 21.5 Ma in connection with the opening of the Ligur-Provencal basin. At the same time, according to [7, 18], this rotation was completed 13–16 million years ago. We add to above mentioned that in [11] the Sicily movement from the central Mediterranean in the northern direction to its current position is demonstrated in the interval 0–35 million years.

At the same time, it remains an open question how was created the Sicily north-eastern extremity which exists to the north-east of the southern tip of the Apennine peninsula at the present day.

The examples show that in the literature there is no consensus on an initial geographic position of Corsica, Sardinia, Sicily, Apennines etc. To restore their possible relative position in the present work a comprehensive paleogeodynamics analysis of the structure of the continental blocks surrounding the basin of the Tyrrhenian Sea is carried out. The basin located between Corsica and Sardinia in the West, Sicily in the South and the Apennine Peninsula in the East and has a triangular shape with a total elongation in longitudinal direction (Figs. 2 and 3). The bottom central part of the basin lies at depths greater than 3 km. The thickness of the continental crust at the periphery of the basin is 25–30 km and dramatically decreases toward its central part, where the continental crust is replaced by discovered by drilling of the ocean crust of 4–5 km [4].



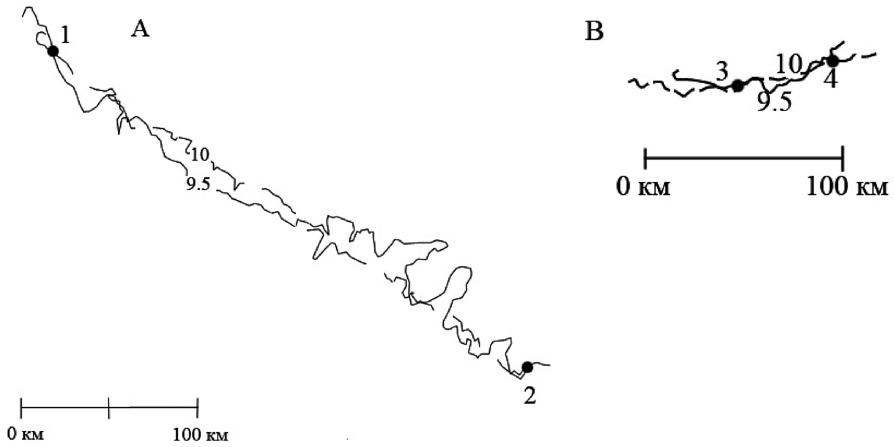


**Fig. 2.** Coinciding of isobaths 1 km on the slopes of the block CS and isobath 0.95 km on the slope of the Apenninian peninsula (A) and Sicily (B). The position of points 1–4 are shown in Fig. 1. Isobaths are in hundreds of meters by [20].

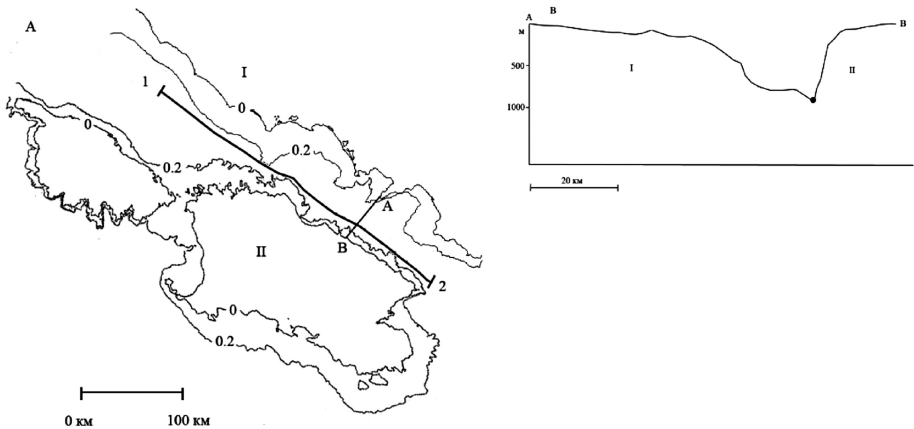


**Fig. 3.** A - Paleogeodynamic reconstruction of the clamping counter-slopes of the Apenninian Peninsula and the block CS. Bold line indicates the restored portion of the zone split axis. The position of the points 1 and 2 is shown in Fig. 1. B - Paleodepth profile before the split along the line A–B and the docking point of isobaths at the intersection of the line A–B and restored split axis along line 1–2. I and II are the same as in Fig. 1.

Here the consolidated crust directly overlaps by sediments of the upper Miocene – lower Pliocene (7–4 my) in the north-west part of the Vavilov basin, or by the sedimentary formations of the upper Pliocene (2–1, 8 my) in the south-east part of Marsili basin. Note that the North Tyrrhenian basin is adjacent to Ligurian basin with bottom depths of up to 2.8 km.

### 3 Calculation of Geodynamic Parameters

In the well-known paper [8] was firstly proposed computational method for the best combination of isobaths bounding the slopes of the continents at the edges of the Atlantic ocean. The combination was carried out by method of trials and errors, by minimizing the angular disagreement, measured along the Eulerian latitudes. The methodology is illustrated the principle that the best alignment can be performed for any of the circuits, as installed, or as expected, once constituted a single circuit. By implementing the principle of better alignment, it is possible to achieve reunification and rehabilitation of the primary continuity of all circuits, including isochronous, isobath, isohypse etc.

According to the electronic Bank on the bottom bathymetry [20] built the profiles in the direction perpendicular to the strike of the Tyrrhenian basin slopes with cross profiles distance of 5–10 miles. Analysis of the profiles indicates that almost all of them consist of three parts (Fig. 4). The upper (shallower than 1.5 km) and lower (deeper 2.9 km) parts of the slopes are no constant along the profile steepness. The Central part of the slopes, enclosed in the depth interval 0.7–1.9 km, is steep and has a relatively constant slope along each individual profile.

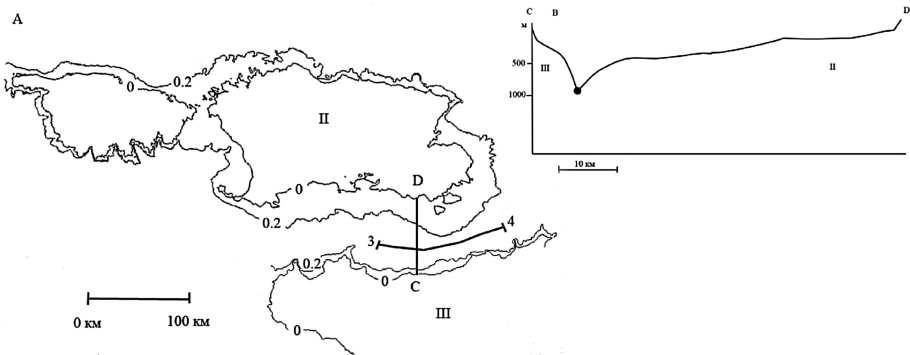


**Fig. 4.** A - Paleogeodynamics reconstruction of clamping of the counter slopes of Sicily and block CS. Bold line indicates the restored portion of the axis of the zone split. The position of points 3 and 4 is shown in Fig. 1. B - Profile bottom paleorelief before the split along the line C–D and the docking point of isobaths at the intersection of the C–D profile and line 3–4 restored split axis. II and III are the same that in Fig. 1.

Sedimentation in different areas of the Tyrrhenian basin has led to them filling in the sedimentary rocks, accompanied by decreasing angle of slopes due to sedimentation process. The sedimentation is uneven in time and space. Irregularity of it is associated with the distribution and redistribution of areas of drift, and with sediment slumping due to loss of stability. Instability precipitation occurs due to the accumulation of a critical mass, leading to slip along the interface or inside the precipitation along the surface of the foundation when varying the steepness of the slope. At small

tilt angles and, *ceteris paribus*, the movement of sedimentary masses down the slope will be very low velocities.

Estimates show that in order to overcome the adhesion force between layers of sediments (in the Tyrrhenian basin is silt, clay, loam sand) and avalanche breakdown them down the slope with the development of considerable (up to close to 50 km/h) velocities of sliding, *ceteris paribus*, the slope of the sliding surface should be less than  $3^\circ$  [2]. Among the reasons for initiating the precipitation from sliding down the slope, is important impact on sediment mass exogenous (regular flow) and endogenous (e.g., earthquake) factors.

Based on the foregoing, in the present work, a modified method of E. Bullard was firstly applied for the case of combining the depth contours of the Tyrrhenian sea basin slopes. Numerous testing the connectivity of different areas different and the same isobaths showed that the most suitable for the purposes of paleogeodynamic analysis were portions of the isobaths in the range of 0.7–1.9 km.

In the depth interval 0.8–1.5 km the continental slope is steepest (the average angle of the slope surface greater than  $100^\circ$ ) and, using the information above about the nature of the sedimentary strata slipping, having the small thickness of sediments (or even completely devoid of them). On this basis, using a modified methodology E. Bullard joined us plots (Fig. 5) the 1 km isobaths on the slope of Sardinia and Corsica and 0.95 km, on the slopes of Sicily and the Apennine peninsula. Calculations of the Euler poles and rotation angles was carried out according to programs incorporated in the software environment, Global Mapper [6] and the principles which are set out in the works [3, 6]. In recent years, in the work [6] develops a methodology of automated selection conjugate plots of depth contours using statistical estimates of the extent of their connectivity.

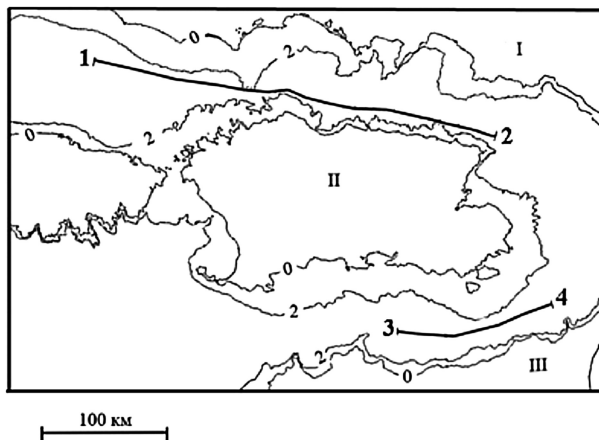


**Fig. 5.** Paleogeodynamic reconstruction of the Tyrrhenian continent. The lines in bold show the recovered split axis of the continent stretching areas. Designations I–III and the position of the points 1–4 are shown in Fig. 1.

## 4 Configuration of the Split Axis

According to the calculations at the position of the Euler poles of finite rotation coordinates  $45.28^\circ$  N  $12.65^\circ$  W manages North of  $40^\circ$  N for about 300 km to get a good combination isobath 0.95 km (section between points 1 and 2 in Fig. 1) the Western slope of the Apennine Peninsula and 1 km isobath (the area between the points 1<sup>1</sup> and 2<sup>1</sup> in Fig. 1) the Eastern slope of the block CS with an error in points of digitization  $\pm 8.7$  km (16 points calculation). The module of the angle of rotation made  $28.79^\circ \pm 0.7^\circ$ . The results of the docking of the isobaths are given in Fig. 2A

At the position of the Euler poles of finite rotation coordinates  $50.45^\circ$  N  $14.76^\circ$  W manages the North 390 North latitude. over 100 km (the section between points 3 and 4 in Fig. 1) get a very good alignment of 0.95 km isobath of the Northern slope of Sicily and the 1 km isobath (the area between points 31 and 41 in Fig. 1) South slope block CS with an error in points of digitization  $\pm 5.4$  km (8 points calculation). The module of the angle of rotation made  $23.57^\circ \pm 0.4^\circ$ . The results of docking the isobaths shown in Fig. 2.

Under the proposed approach, the combined plots of depth contours 1 km from the side of block KS and 0.95 km from the Apennine Peninsula (Fig. 3A) and from the side of Sicily (Fig. 4A) allow us to restore the planned configuration of the axes of the zones of continental rifting, which was the consequence of the processes of stretching. Docking of isobaths discussed above allows us to represent the profiles of the upper surface of the neck stretching of the continental crust immediately prior to rupture of the lithosphere and the initialization is split between the Apennine Peninsula and block CS (Fig. 3B), as well as Sicily and CS (Fig. 4B). These profiles show that the region of stretching in both cases had a width of over 150 km, and was more steep in the direction of the CS in the first case and in the direction of Sicily in the second.

The experimental data obtained are important for the recovery of process parameters of the rupture of the continental crust during rifting of the lithosphere in the Western Mediterranean. Splits the continental lithosphere in rifts could occur according to the scheme of Wernicke [19]. Listric quasilinear with sloping fault that separates the plates and reaches the surface, forming a separation zone “hanging” plate from the “underlying”.

The result of the paleogeodynamic reconstruction is to restore the split axis of the chipping peripheral areas of the CS block from the Apenninian peninsula and from Sicily. An important factor of reconstruction is the difference of the abutting 0.05 km the latter fact probably reflects the circumstance of sliding along the lithospheric fault plane and downgliding in the process of stretching peripheral areas of the continental crust CS from the peripheral regions of Sicily and the Apennines in accordance with modification Schreider [6] scheme of Wernicke [19].

## 5 Paleogeodynamics of the Tyrrhenian Continent Split

Integrated geophysical analysis of available materials shows that paleogeodynamics evolution of the Western Mediterranean resulted in the formation of the Miocene continental array in place of the modern Tyrrhenian sea. Calculations of the Euler poles

and rotation angles for the first time allowed to restore the position of the split axis of the stretched zone between the CS and the Apennines (Fig. 3) and the other split axis of the stretched zone between the CS and Sicily (Fig. 4). Joint analysis of two independent reconstructions allowed for the first time to make a general reconstruction of the Tyrrhenian continent (Fig. 5), which initially consisted of the Islands of Corsica, Sardinia, Sicily, parts of the Apennine peninsula. In the process of its destruction formed the basin of the Tyrrhenian sea - the youngest in the Western Mediterranean basins. Basin began to develop [5, 14, 17] in the late Miocene, about 9 million years ago when continental destruction has led to the emergence of the deep Vavilov basin. The pool continued to evolve until the turn of 4 million years ago, and after a break of 2 million years to the South-East it occurred the opening of the Marsili basin [4, 5], development of which is still ongoing. The sea floor spreading in the Tyrrhenian sea was diffuse [1, 5, 14, 17] and spread from North-West to South-East in several areas, which has created an extremely complex structure closed at present, precipitation of the consolidated crust in the form of horst and grabens, superimposed on the under crust.

**Acknowledgement.** The work was done in the framework of the State assignment, project 0149-2018-0015. While methodological issues of combining conjugate isobaths was supported by the Russian Foundation for Basic Research Project № 17-05-00075.

## References

1. Verzbitsky, E.V., Schreider, A.A., Stenshinsky, S.B.: Diffusive spreading rates in the Tyrrhenian sea. *Izv. Ross. Akad. Nauk, Ser. Geol.* **55**(8), 53–64 (1992). [in Russian]
2. Zhmur, V.V., Sapov, D.A., Nechaev, I.D., et al.: Intensive gravitational currents in the near bottom layer of the ocean. *Izv. Ross. Akad. Nauk, Ser. Fiz.* **66**(12), 1721–1726 (2002). [in Russian]
3. Zonenshtein, L.P., Lomize, M.G., Ryabukhin, A.G.: Practical Manual on Geotectonics. Moscow State University, Moscow (1990). [in Russian]
4. Khain, V.Y.: Tectonics of the land and ocean. Nauchnyi Mir, Moscow (2001)
5. Khain, V.Y., Limonov, A.F.: Regional geotectonics. Geos, Moscow (2004). [in Russian]
6. Schreider, Al.A.: Formation of the Black Sea deep basin. Nauchnyi Mir, Moscow (2011). [in Russian]
7. Argnani, A., Savelli, C.: Cenozoic volcanism and tectonics in the southern Tyrrhenian sea: space-time distribution and geodynamic significance. *Geodynamics* **27**, 409–432 (1999)
8. Bullard, E., Everett, J., Smith, A.: The fit of continents around Atlantic. *Philos. Trans. Roy. Soc. Lond.* **258A**, 41–51 (1965). Symposium on Continental Drift
9. Faccenna, C., Becker, W., Lucente, P., Joliet, L.: History of subduction and back arc extension in the central Mediterranean. *Geophys. J. Int.* **145**, 809–820 (2001)
10. Gattacceca, J., Deino, A., Rizzo, R., et al.: Miocene rotation of Sardinia: new paleomagnetic and geochronological constraints and geodynamic implications. *Earth Planet. Sci. Lett.* **258**, 359–377 (2007)
11. Goes, S., Giardini, D., Jenny, S., et al.: A recent tectonic reorganization in the south-central Mediterranean. *Earth Planet. Sci. Lett.* **226**, 335–345 (2004)
12. Handy, M., Schmid, S., Bouscquet, R., et al.: Reconciling plate-tectonic reconstructions of Alpine Tethys with the geological-geophysical record of spreading and subduction in the Alps. *Earth Sci. Rev.* **102**, 121–158 (2010)

13. Maffione, M., Speranza, F., Faccenna, C., et al.: A synchronous Alpine and Corsica-Sardinia rotation. *J. Geophys. Res.* **113**, 25–35 (2008)
14. Savelli, C., Schreider, A.A.: The opening processes in the deep Tyrrhenian basins of Marsili and Vavilov, as deduced from magnetic and chronological evidence of their igneous crust. *Tectonophysics* **190**, 119–131 (1991)
15. Scalera, G.: The Mediterranean as a slowly nascent ocean. *Ann. Geophys. Suppl.* **49**, 451–482 (2006)
16. Scheepers, P., Langereis, C., Zijdeveld, J., Hilgen, F.: Paleomagnetic evidence for a Pleistocene clockwise rotation of the Calabro-Peloritan block (southern Italy). *Tectonophysics* **230**, 19–48 (1994)
17. Schreider, A.A., Yastrebov, V.S., Rimsky-Korsakov, N.A., Savelli, C.: Indagini e campionature di dettaglio di affioramenti rocciosi submarini dei Monti Baronie (Mar Tirreno): Primi risultati. *Mem. Soc. Geol. It.* **36**, 91–98 (1988)
18. Speranza, F., Villa, I., Sagnotti, L., et al.: Age of the Corsica-Sardinia rotation and Liguro-Provençal basin spreading: new paleomagnetic and Ar/Ar evidence. *Tectonophysics* **347**, 231–251 (2002)
19. Wernicke, B.: Low angle normal faults in the Basin and Range Province: nappe tectonics in an extending orogeny. *Nature* **291**, 645–648 (1981)
20. [ftp://topex.ucsd.edu/pub/srmt15\\_plus/](ftp://topex.ucsd.edu/pub/srmt15_plus/)



# Long Waves Influence on Polarization Ratio for Microwave Backscattering from the Sea Surface

Alexandr Zapevalov<sup>(✉)</sup> 

Marine Hydrophysical Institute RAS, Sevastopol 299011, Russia  
sevzepter@mail.ru

**Abstract.** The effect of slopes created by long waves on the resonance backscattering of microwave radio waves analyzed. The analysis is carried out within the framework of the Gaussian model of slopes distribution. The polarization ratio increases by approximately 10% as the wind speed increases up to 5 m/s if the sounding is performed along the direction of wind. If the sensing is accomplished across the direction of wind, as the wind speed tends to 5 m/s the polarization ratio increases to approximately 6%. The effect of the presence of long waves weakly depends on the incidence angle.

**Keywords:** Remote sensing · The microwave radiation · Resonance scattering  
Polarization ratio · Sea surface · Long waves

## 1 Introduction

The number of oceanographic spaceborne microwave sensors is continuously growing. Expands the range of parameters determined on the basis of data of remote sensing of the ocean. All this requires a detailed understanding of the characteristics of electromagnetic fields scattered by sea surface.

Models of the normalized radar cross-section of sea surface at incidence angles between 25° and 70° are usually treated as resonant (Bragg) scattering mechanism [1]. The resonance condition relates the wave number of radio wave and surface wave [2]

$$K_R = 2k \sin \theta, \quad (1)$$

where  $K_R$  is the wave number of surface resonance waves,  $k$  is the radar wave number,  $\theta$  is the incidence angle.

If the resonant waves propagate along the flat surface, the normalized radar cross-section is proportional to the surface elevation spectrum at the resonance wave number [3, 4]

$$\sigma_{pp}^0 = 8\pi k^4 |G_{pp}(\theta)|^2 [\Psi(\vec{K}_R) + \Psi(-\vec{K}_R)], \quad (2)$$

where  $pp$  is the polarization (the first index corresponds to emitted wave, the second one does to be received),  $|G_{pp}(\theta)|^2$  is the polarization dependent reflection coefficient,

$\Psi(\vec{K}_R)$  is the two-dimensional (Cartesian) wave-number spectrum of sea surface displacement. Resonance scattering of radio waves create surface waves traveling along the direction of sensing in forward or reverse direction. In this case, the polarization ratio

$$R^0(k, \theta) = \sigma_{HH}^0(k, \theta) / \sigma_{VV}^0(k, \theta) \quad (3)$$

is described by the expression

$$R^0(k, \theta) = |G_{HH}(\theta)|^2 / |G_{VV}(\theta)|^2. \quad (4)$$

It should be noted that the polarization ratio (4) does not depend on the level of the sea surface roughness. This gives a fundamental possibility of remote determination of physical and chemical characteristics (temperature, salinity) of sea water. The presence on the sea surface waves longer than resonant waves modifies expression (2) [5]. Resonant waves propagate along the curved surface. The local incidence angle  $\theta$  changes. As the result, the resonance condition (1) changes as well as the value of the spectrum  $\Psi(\vec{K}_R)$  changes. Accordingly, the polarization ratio changes.

The main objective of this work is an analysis of the impact of long surface waves on polarization ratio. Long waves are waves with lengths much greater than the length of resonant waves.

## 2 Normalized Radar Cross-Section in the Presence of Long Waves

We assume that the size of radar spot on sea surface significantly exceeds the size of long waves. In this case, the effect of long waves on the backscattered signal can be taken into account by averaging expression (2) over the entire range of their slopes. Within the frame of the two-scale model, where resonant waves superposed on longer tilting waves in [3] obtained

$$\sigma_{pp}^L = 8\pi k^4 \int |G_{pp}(\theta, \delta)|^2 [\Psi(\vec{K}_R) + \Psi(-\vec{K}_R)] P(\xi_x, \xi_y) d\xi_x d\xi_y, \quad (5)$$

where  $\delta$  is the out-of-plane tilt angle,  $\xi_x$  and  $\xi_y$  are orthogonal components of sea surface slope,  $P(\xi_x, \xi_y)$  is the two-dimensional probability density function of slopes. Physically (5) is the averaging with the weight being proportional to  $P(\xi_x, \xi_y)$  (the expected tilt of long waves).

The slopes  $\xi$  and their angles  $\beta$  are related by the nonlinear expression

$$\xi = \tan \beta. \quad (6)$$

Usually it was assumed that the slopes are small and one can use approximation  $\xi \approx \beta$ . An analysis of the errors associated with this approximation was carried out in [6].



It was shown that the variance slopes is of 8% higher than the variance of angles. The discrepancies for the higher statistical moments are higher. As a consequence, the probability density function of slopes, which is described using the Gram-Charlier series [7], differs significantly from the probability density function of angles.

We use a model in which the approximation  $\xi \approx \beta$  is not used. This model has the form

$$\sigma_{pp}^L = \int \sigma_{pp}^0(k, \theta - \beta_{\uparrow}, \alpha) P(\beta_{\uparrow}) d\beta_{\uparrow}, \quad (7)$$

where  $\beta_{\uparrow}$  is the angle of inclination of the sea surface in the direction of sounding,  $\alpha$  is azimuth angle. To realize averaging (7), the spectrum of sea surface elevation represented as an explicit function of the incidence angle is required. The transition is carried out by using the normalization condition. According to this condition, the integral of the evaluation spectrum of elevations in all its variables is equal to the variance of elevations. In final form (6) received [5]

$$\sigma_{pp}^L = 2\pi k^2 \int |G_{pp}(\theta_{\beta})|^2 \frac{S(2k \sin \theta_{\beta})}{\sin \theta_{\beta} \cos \theta_{\beta}} \Theta(k2 \sin \theta_{\beta}, \alpha) P(\beta_{\uparrow}) d\beta_{\uparrow}, \quad (8)$$

where  $\theta_{\beta} = \theta - \beta_{\uparrow}$ ,  $S$  is the one-dimensional wave-number spectrum of the sea surface displacement,  $\Theta$  is the directional spreading function. The function  $\Theta$  describes the angular distribution of wave energy. This function satisfies the normalization condition  $\int_{-\pi}^{\pi} \Theta(\alpha) d\alpha = 1$ .

In the general form, the coefficient  $|G_{pp}(\theta)|^2$  depends on the relative dielectric constant of sea water. If the sounding is carried out in the centimeter range of the radio wave, we can use the simplified form proposed in the paper [8]. A simplified form is obtained under the assumption that the dielectric constant of sea water be equal to 81. For the vertical  $VV$  and horizontal  $HH$  polarizations, the coefficients  $|G_{VV}(\theta)|^2$  and  $|G_{HH}(\theta)|^2$  have the forms

$$|G_{VV}(\theta)|^2 = \frac{\cos^4 \theta (1 + \sin^2 \theta)^2}{(\cos \theta + 0.111)^4}, \quad (9)$$

$$|G_{HH}(\theta)|^2 = \frac{\cos^4 \theta}{(0.111 \cos \theta + 1)^4}. \quad (10)$$

We assume that long compared to resonance waves are longer than 20 cm. It is usually assumed that waves are long, if their length is 3–4 times greater than the length of the sensing radio waves. According to [9, 10], the variance of the slopes generated by these waves is approximately 1/3 of the total variance of slopes. Up/down wind  $D(\xi_u)$  and crosswind  $D(\xi_c)$  variance of slopes were determined from optical measurements [11]

$$D(\xi_u) = 0.000 + 0.00316W \pm 0.004, \quad (11)$$

$$D(\xi_c) = 0.003 + 0.00192W \pm 0.002, \quad (12)$$

where  $W$  is wind speed at a height 10 m. Variances of slopes and angles are related as  $D(\beta) = 0.92D(\xi)$  [6]. Here and further, the indices “ $u$ ” and “ $c$ ” correspond to directions up/down and cross wind. If the expression applies to both up/down and cross wind components of the slopes, the subscript is missing.

The wind speed dependences for standard deviation angles  $\beta$  ( $\text{rms}(\beta)$ ) obtained in this way are shown in Fig. 1. The same figure shows the similar dependence, obtained according to measurements of wind speed and direction from the NASA Scatterometer and ocean reflectance from the POLDER (POLARization and Directionality of the Earth Reflectances) multi-directional radiometer [12].

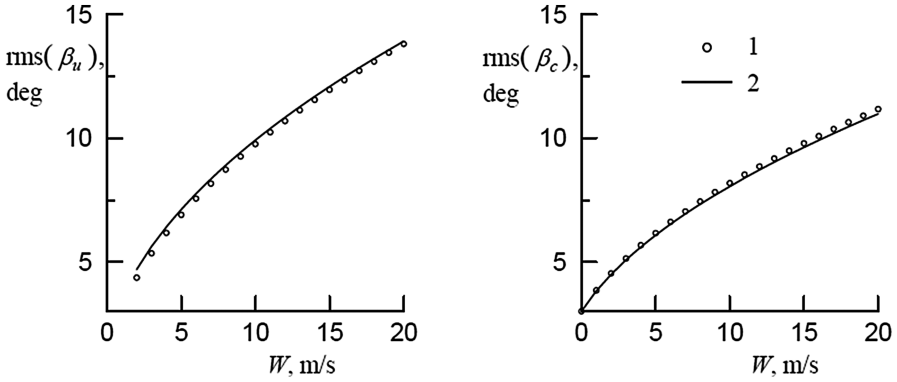


**Fig. 1.** The dependence for standard deviation angles  $\text{rms}(\beta)$  on wind speed  $W$ . Curve 1 is constructed according to [11], curve 2 – according to [12]

We introduce the non-dimensional parameter

$$\chi_{pp}(\theta, W) = \sigma_{pp}^L / \sigma_{pp}^0 \quad (13)$$

which describes influence of long waves on normalized radar cross-section. We also assume that the angles  $\beta$  have a Gaussian distribution. The dependence of the parameter  $\chi_{pp}$  on the incidence angle is shown in Fig. 2.

The dependencies  $\chi_{pp} = \chi_{pp}(\theta)$  shown in Fig. 2 are constructed for three wind speeds. It can be seen that the effect of slopes produced by long waves is more pronounced on vertical polarization than on horizontal polarization.

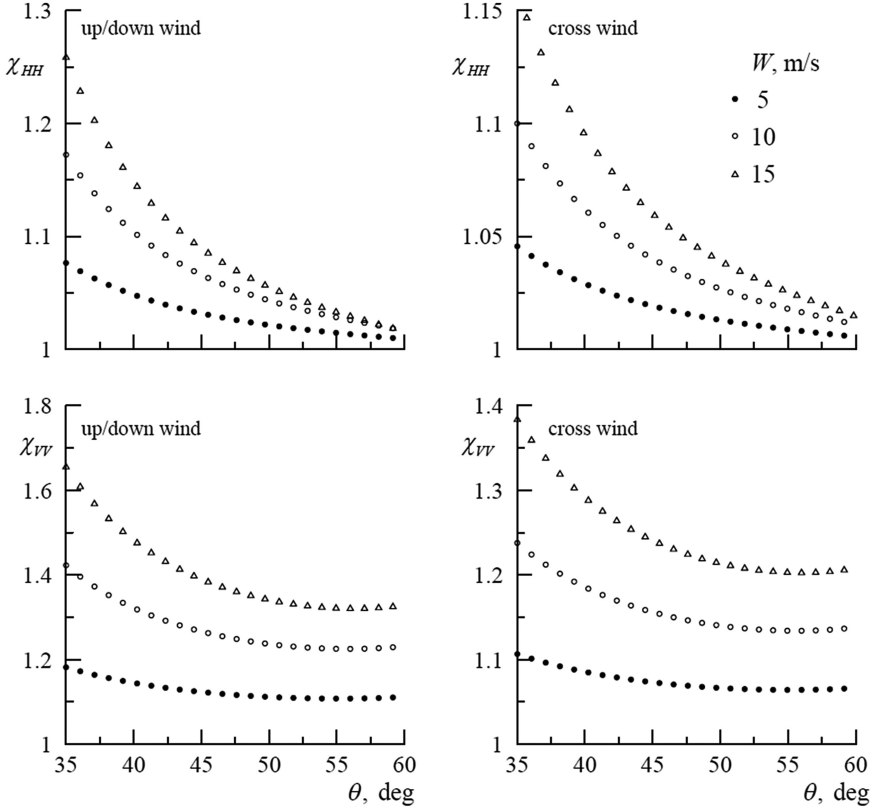


Fig. 2. The dependence of radar cross-section  $\chi_{pp}$  on wind speed  $W$

### 3 Polarization Ratio in the Presence of Long Waves

In the presence of long waves the polarization ratio can be represented in the form

$$R^L = \frac{\sigma_{HH}^L}{\sigma_{VV}^L} = \frac{\int |G_{HH}(\theta_\beta)|^2 \frac{S(2k \sin \theta_\beta)}{\sin \theta_\beta \cos \theta_\beta} \Theta(k2 \sin \theta_\beta, \alpha) P(\beta_\uparrow) d\beta_\uparrow}{\int |G_{VV}(\theta_\beta)|^2 \frac{S(2k \sin \theta_\beta)}{\sin \theta_\beta \cos \theta_\beta} \Theta(k2 \sin \theta_\beta, \alpha) P(\beta_\uparrow) d\beta_\uparrow}. \quad (14)$$

Polarization ratios (14) predicted by multiscale composite models based on the resonance theory scattering models that include the effects of long-wave tilt.

Directional spreading function is the narrowest on the scale of the dominant waves [13]. As the wave number increases, it expands. In the range of gravity-capillary waves the angular distribution of wave energy become isotropic. This suggests that the change in the length of the resonant waves do not lead to significant changes in the function of angular distribution and we can eliminate the function  $\Theta(2k \sin \theta_\beta, \alpha)$  in (14).

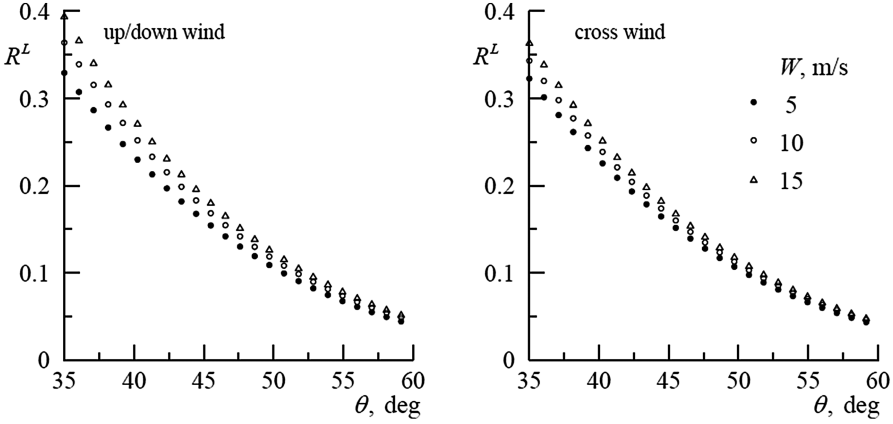


**Fig. 3.** The dependence of the polarization ratio  $R^L$  on the angle of incidence  $\theta$  and the wind speed  $W$

Graphs on Fig. 3 are obtained within assumption that waves of the gravitational-capillary range are resonant. According to [14], in this range the spectrum of surface waves is approximated by the dependence

$$S(K) \sim K^{-3}. \tag{15}$$

In order to quantify the change in the polarization ratio with the change in wind speed, we investigate the parameter

$$\psi(\theta, W) = R^L/R^0, \tag{16}$$

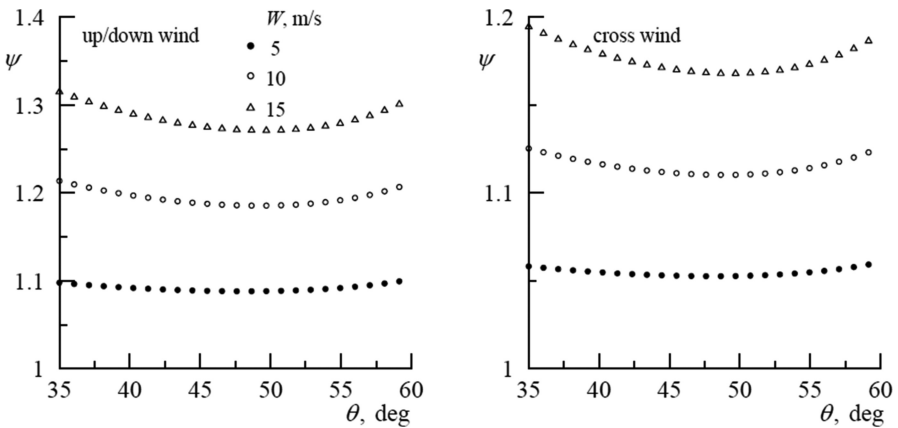


**Fig. 4.** The dependence of the parameter  $\psi$  on the angle of incidence  $\theta$  and wind speed  $W$

where  $R^0 = \sigma_{HH}^0 / \sigma_{VV}^0$ . The parameter  $\psi$  describes the change in polarization relations compared to the situation when the resonance waves propagate along the flat surface. How the parameter  $\psi$  changes when the wind speed or the incidence angle change is shown in Fig. 4.

## 4 Conclusion

An analysis of the effect of long surface waves on the field of backscattered radio waves, when sounding the sea surface in the microwave range is made. The situation is considered when resonant scattering is the dominant mechanism of creating a scattered field. The calculations were performed for incidence angles from  $35^\circ$  to  $60^\circ$ . With wind speed increasing at 5 m/s, the polarization ratio increases by approximately 10% if the sounding is performed along the wind direction. If the sounding is performed across the wind direction, then with wind speed increase at 5 m/s, the polarization ratio is increased approximately on 6%. The effect of the presence of long waves weakly depends on the incidence angle.

**Acknowledgements.** This work was carried out in the context of the State project № 0827-2014-0011.

## References

1. Valenzuela, G.: Theories for the interaction of electromagnetic and ocean waves - a review. *Bound. Layer Meteorol.* **13**(1–4), 61–85 (1978)
2. Bass, F.G., Fuchs, I.M.: *Wave Scattering from Statistically Rough Surfaces*. Pergamon Press, Oxford (1978)
3. Thompson, D., Elfouhaily, T., Chapron, B.: Polarization ratio for microwave backscattering from the ocean surface at low to moderate incidence angles. In: *Proceedings of the 1998 IEEE International Geoscience and Remote Sensing Symposium, IGARSS 1998*, pp. 1671–1673. IEEE, Seattle (1998)
4. Kudryavtsev, V., Hauser, D., Caudal, G., Chapron, B.: A semiempirical model of the normalized radar cross-section of the sea surface I. Background model. *J. Geophys. Res.* **108** (C3), 8054 (2003). <https://doi.org/10.1029/2001JCOO1003>
5. Zapevalov, A.S.: Bragg scattering of centimeter electromagnetic radiation from the sea surface: the effect of waves longer than Bragg components. *Izv. Atmos. Ocean Phys.* **45**(2), 253–261 (2009)
6. Zapevalov, A.S., Lebedev, N.E.: Simulation of statistical characteristics of sea surface during remote optical sensing. *Atmos. Ocean. Opt.* **27**(6), 487–492 (2014)
7. Zapevalov, A.S., Pustovoitenko, V.V.: Modeling of the probability distribution function of sea surface slopes in problems of radio wave scattering. *Radiophys. Quantum Electron.* **53** (2), 100–110 (2010)
8. Plant, W.J.: A two-scale model of short wind-generated waves and scatterometry. *J. Geophys. Res.* **91**, 10735–10749 (1986)
9. Hollinger, J.P.: Passive microwave measurements of sea surface roughness. *IEEE Trans. Geosci. Electron. (GE)* **9**, 165–169 (1971)

10. Wilheit, T.T.: A model for the microwave emissivity of the ocean's surface as a function of wind speed. *IEEE Trans. Geosci. Electron. (GE)* **17**(4), 244–249 (1979)
11. Cox, C., Munk, W.: Measurements of the roughness of the sea surface from photographs of the sun glitter. *J. Opt. Soc. Am.* **44**(11), 838–850 (1954)
12. Bréon, F.M., Henriot, N.: Spaceborne observations of ocean glint reflectance and modeling of wave slope distributions. *J. Geoph. Res.* **111**(56), 1–10 (2006). C06005
13. Zapevalov, A.S.: On the estimation of the angular energy distribution function of dominant sea waves. *Izv. Atmos. Ocean Phys.* **31**(6), 802–808 (1996)
14. Monin, A.S., Krasitskii, V.P.: *Phenomena on the Ocean Surface*. Gidrometeoizdat, Leningrad (1985). [in Russian]